# A Novel Generalized Analytical Framework to Diagnose True Radial and Axial Displacements in an Actual Transformer Winding


**Pritam Mukherjee and L. Satish**

Department of Electrical Engineering, Indian Institute of Science, Bangalore.

e-mail: mukherjee.hve@gmail.com


## 1 Introduction

A mechanical damage of the winding is the end-result of accumulated strains from abnormal forces experienced by the winding due to short-circuits in the nearby power network. In the initial stages, often the damage is conned to a small physical portion of the winding. But, the winding will need a complete replacement if the initial damage (when left unattended) is allowed to reach the final stage, and that must be prevented at all costs. Hence, detection of damage at the very early stage of evolution is paramount.

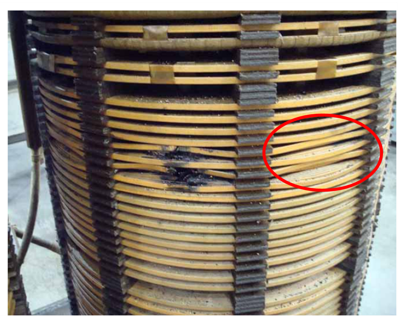

Fig. 1: Winding damage

## 2 FRA: monitoring and diagnostics

Frequency Response Analysis (FRA) is, perhaps, the most sensitive means for checking the mechanical integrity of the iron core and winding assembly. A mismatch between two FRAs in the range of 10kHz - 1MHz would indicate a damage in the winding structure. Once a mechanical damage is confirmed by FRA, the next logical step would be to determine, if possible, its severity and also know where it is located along the winding. Unfortunately, even though FRA has been in use for almost 25 years, not much progress has been achieved in this direction.

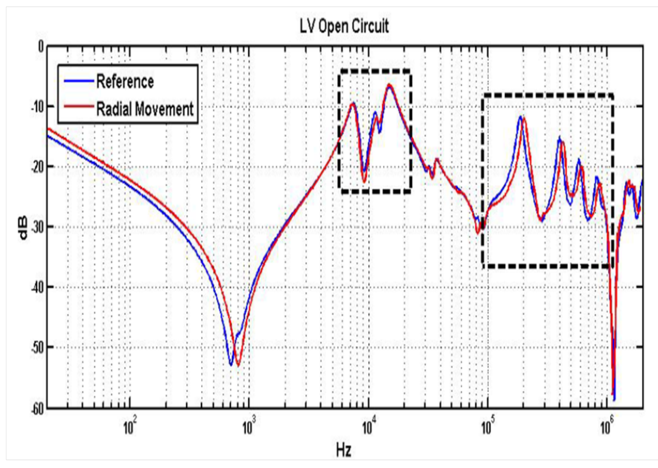


Fig. 2: FRA comparison

## 3 Scope of the work and Objectives

- A single, actual, isolated, air-cored, continuous-disk transformer winding is considered. Actually, in practice, it is possible to limit the influence of the core and neighbouring windings by choosing proper terminal connection.
- Different types of damages have varying types of influence on the inductances and capacitances. The axial and radial displacements are completely independent of each other and all other damages can possibly be visualized as a combination of these two types. Hence, axial and radial displacements need to be addressed first.
- The radial displacements and axial displacements considered are in their infancy since, early diagnosis of mechanical damages is the goal of FRA measurement.

The objectives of this thesis were formulated as

- Initially, derive an analytical expression to correlate changes in natural frequencies to the changes in the ladder network (in which each section is distinct).
- Extend the formulation from discrete-domain (ladder network) to continuous-domain (actual winding)
- Finally, use this formulation to (i) locate true radial and axial displacements in an actual transformer winding and, (ii) also estimate their severities Achieving these objectives shall be subject to the condition that only inputs that are readily measurable from the terminals, and data related to the winding in its nominal state, shall be used.

## 4 Used model

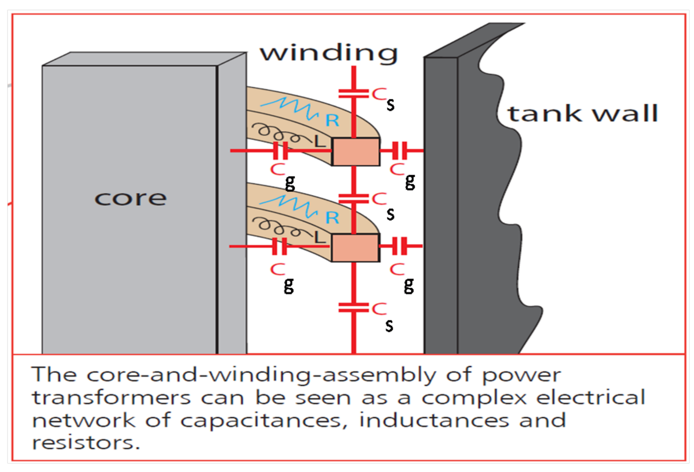


Fig. 3: Origin of the equivalent circuit

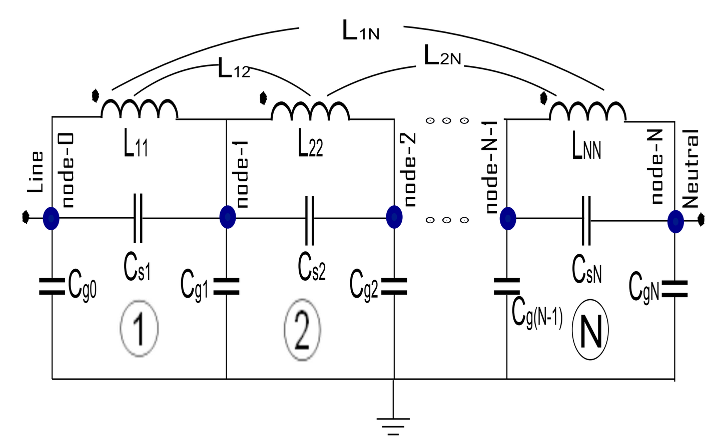


Fig. 4: $N$-section fully mutually coupled ladder network

## 5 Theoretical formulation

The relationship between natural frequencies and the network parameters were derived staring from the state-space representation of a fully mutually-coupled ladder network

$$\Psi_{scnf} = \sum_{i=1}^{N} 1/\omega_{sc_i}^2 = \sum_{i=1}^{N} L_{ii}C_{si} + \sum_{i=1}^{N} \mathrm{M}_{0i}C_{g_i} \qquad (1)$$

$$\sum_{i=1}^{N} \frac{1}{\omega_{oc_i}^2} = \sum_{i=1}^{N} L_{ii}C_{si} + \frac{1}{C_G} \sum_{i,j=1, i\neq j}^{N} \mathrm{M}_{ij}C_{g_i}C_{g_j} \qquad (2)$$

where, $L_{ii}$ : self inductance of $i^{\text{th}}$-section, $L_{ij}$ : mutual inductance between $i^{\text{th}}$-$j^{\text{th}}$ section, $C_{s_i}$ : series capacitance of $i^{\text{th}}$ section, $C_{g_i}$ : ground capacitances, $\mathrm{M}_{0i}$ : Total inductance between the line-end and $i^{\text{th}}$ disk, $\mathrm{M}_{ij}$ : Total inductance between $i^{\text{th}}$-$j^{\text{th}}$ disk.

## 6 Radial Displacement

A localized RD causes a localized change in ground capacitance only. Following an RD in the mth section, the change in the SCNFs is given by

$$\Delta\Psi_{scnf} = \sum_{i=1}^{N} 1/\widehat{\omega}_{sc_i}^2 - \sum_{i=1}^{N} 1/\omega_{sc_i}^2 = \mathrm{M}_{0m}\Delta C_g \qquad (3)$$


Fig. 5: Experimental setup


Fig. 6: The winding - after RD

The FRA reveals five SCNFs.
$\Delta\Psi_{scnf} = 6.53 - 5.61 = 0.92$.
The equivalent ground capacitances before and after the introduction of the displacement are 0.389 nF and 0.436 nF respectively. $\Delta C_G = 0.047\ nF$.
Now, $\mathrm{M}_{0f} = \Delta\Psi_{scnf}/\Delta C_g = 19.62\ mH$.
$\mathrm{M}_{0f} = 19.6227$, corresponds to $x_f = 10.7$.

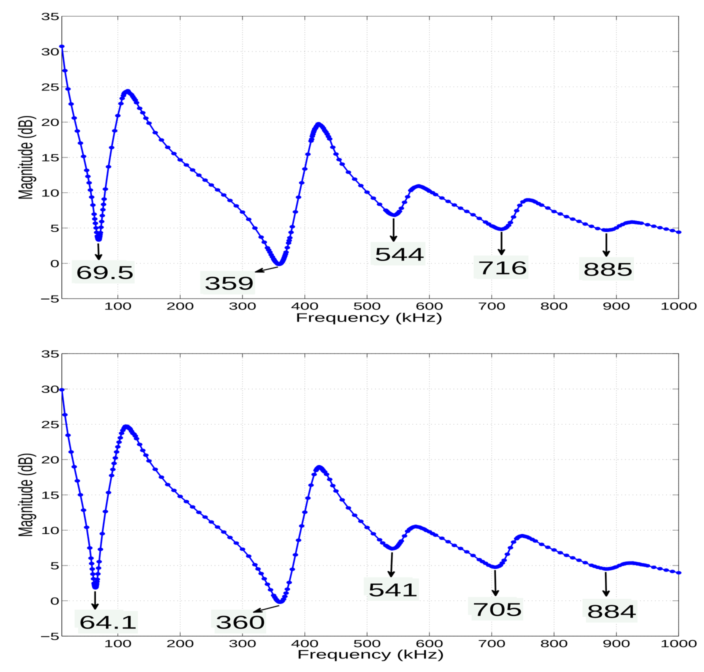


Fig. 7: Measured DPI of nominal (top) and radially displaced (bottom) winding

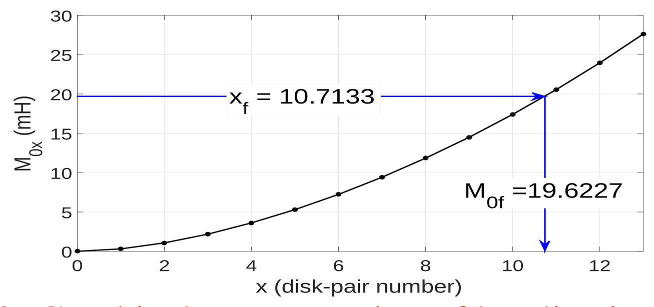


Fig. 8: Graphical representation of localization

| Disk pair | extent (mm) | SCNFs (kHz) | | | | | $\Delta\Psi_{scnf}$ |
|---|---|---|---|---|---|---|---|
| | | $1^{\text{st}}$ | $2^{\text{nd}}$ | $3^{\text{rd}}$ | $4^{\text{th}}$ | $5^{\text{th}}$ | |
| 4 | 3 | 69.1 | 354 | 536 | 718 | 886 | 0.0687 |
| 4 | 4 | 68.8 | 348 | 531 | 718 | 888 | 0.1236 |
| 4 | 5 | 68.5 | 345 | 529 | 718 | 886 | 0.1751 |
| 7 | 3 | 68.6 | 354 | 548 | 714 | 889 | 0.1428 |
| 7 | 4 | 67.6 | 346 | 547 | 710 | 888 | 0.3137 |
| 7 | 5 | 67.2 | 345 | 548 | 707 | 888 | 0.3812 |
| 10 | 3 | 68 | 362 | 541 | 715 | 889 | 0.2315 |
| 10 | 4 | 66.7 | 361 | 536 | 714 | 889 | 0.4499 |
| 10 | 5 | 65.7 | 361 | 535 | 713 | 888 | 0.6251 |
| 10 | 6 | 63.7 | 359 | 533 | 712 | 886 | 1.0025 |

Table I: Proportionality of $\Delta\Psi_{scnf}$ w.r.t. severity/extent of radial displacement

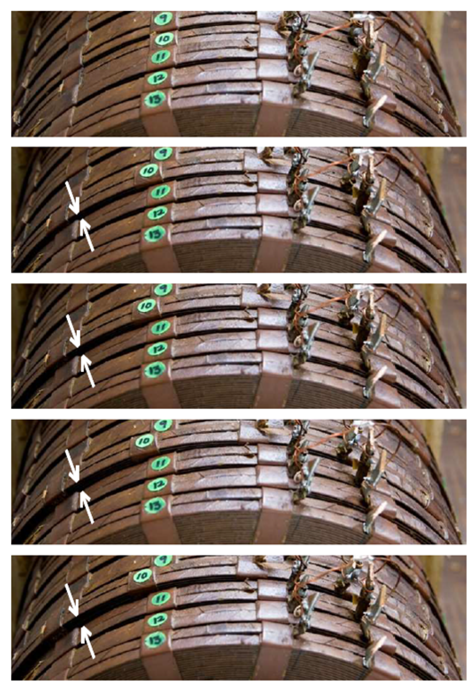

Fig. 9: Varied extent of RD

## 7 Axial Displacement

The same principle is valid for axial displacements too - $\Delta\Psi_{scnf}$ varies monotonically w.r.t. the location and severity.

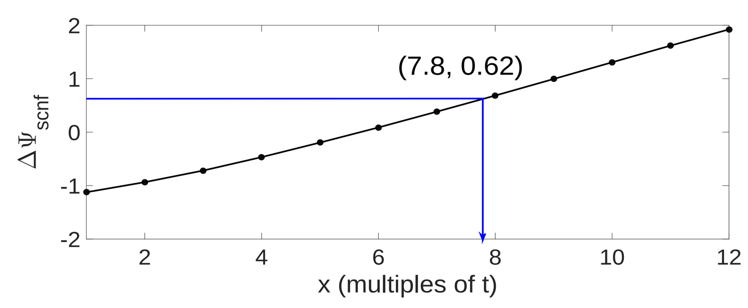


Fig. 10: Localization of AD

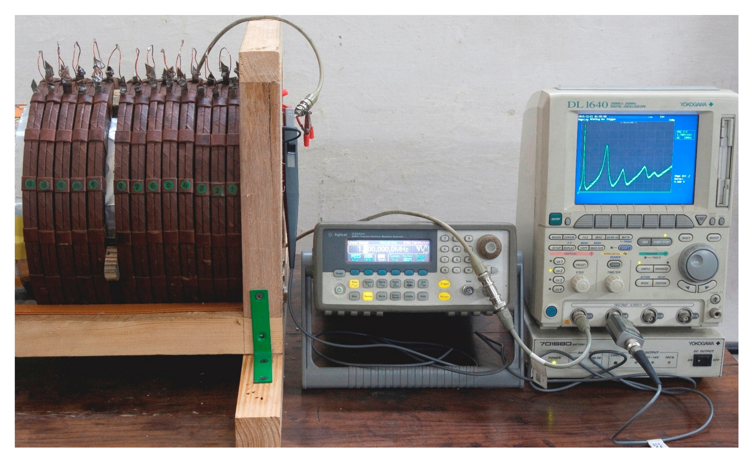

Fig. 11: Experimental setup showing AD

| AD between | $\delta$ (cm) | SCNFs (kHz) | | | | | $\Delta C_g$ (nF) | $\Delta L_{eq}$ (mH) | Location achieved | Estimated $\delta$ (cm) |
|---|---|---|---|---|---|---|---|---|---|---|
| | | $1^{\text{st}}$ | $2^{\text{nd}}$ | $3^{\text{rd}}$ | $4^{\text{th}}$ | $5^{\text{th}}$ | | | | |
| D4-D5 | 0.6 | 42.3 | 283 | 482 | 694 | 862 | 0.047 | -0.55 | 5.7 $\Rightarrow$ D5-D6 | 0.31$t$=0.52 |
| | 1.4 | 42.4 | 278 | 473 | 700 | 845 | 0.075 | -1.03 | 5.9 $\Rightarrow$ D5-D6 | 0.60$t$=1.01 |
| | 2.0 | 42.4 | 275 | 470 | 695 | 842 | 0.087 | -1.68 | 5.8 $\Rightarrow$ D5-D6 | 1.03$t$=1.74 |
| D9-D10 | 0.6 | 42.0 | 287 | 477 | 684 | 870 | 0.038 | -0.59 | 8.5 $\Rightarrow$ D8-D9 | 0.33$t$=0.56 |
| | 1.4 | 41.5 | 289 | 461 | 681 | 870 | 0.058 | -1.13 | 9.1 $\Rightarrow$ D9-D10 | 0.73$t$=1.24 |
| | 2.0 | 41.1 | 288 | 455 | 678 | 870 | 0.092 | -1.78 | 8.5 $\Rightarrow$ D8-D9 | 1.10$t$=1.85 |

Table II: Results for AD with varying extent at different positions

## 8 Conclusions and scope of future work

- For the first time natural frequencies and the winding parameters of a completely inhomogeneous ladder network have been analytically connected. The derived relationships are applicable for all types of winding - damaged or healthy, uniform or non-uniform, continuous-disk type or interleaved. The obtained formulae are new results in circuit theory.
- $\Delta\Psi_{scnf}$ captures the information regarding the location and the severity of damage in a well-understood and easily extractable form. Thus, for the first time, diagnosis of damages from FRA data becomes possible in an analytical framework.
- The future work will make use of the OCNFs and also investigate more complex types of deformations.